Available online at www.sciencedirect.com
ScienceDirect
J. Mater. Sci. Technol., 2012, 28(5), 467–473.
JMST
www.JMST.org

Dynamic Recrystallization Behavior of 13%Cr Martensitic Stainless Steel under Hot Working Condition

G.R. Ebrahimi[1)†], *H. Keshmiri*[2)], *A.R. Maldar*[2)] *and A. Momeni*[3)]
1) Metallurgical and Materials Engineering Department, Ferdowsi University of Mashhad, Mashhad 9177948974, Iran
2) Department of Materials Engineering, Sabzevar Tarbiat Moallem University, Sabzevar 9617976487, Iran
3) Materials Science and Engineering Department, Hamedan University of Technology, Hamedan 6516913418, Iran
[Manuscript received March 15, 2011, in revised form December 7, 2011]

In this study, the effect of hot deformation on martensitic stainless steel was carried out in temperatures between 950 to 1100 °C and strain rates of 0.001, 0.01 and 0.1 s^{-1}. Two important dynamic recrystallization parameters, the critical strain and the point of maximum dynamic softening, were derived from strain hardening rate *vs* stress curves. Then the calculated parameters were used to predict the dynamic recrystallized fraction. Our results show that critical stress and strain increase with decreasing deformation temperature and increasing strain rate. The hot deformation activation energy of the steel is also investigated in the present work with 413 kJ/mol. Our experimental flow curves are in fair agreement with the kinetics of dynamic recrystallization model.

KEY WORDS: Hot deformation; Dynamic recrystallization; Critical strain

1. Introduction

Dynamic recrystallization (DRX) is a microstructural phenomenon which occurs during straining of low-stacking fault energy (SFE) metals at high temperatures. It is characterized by the nucleation and growth of new grains at pre-existing grain boundaries and produces a homogeneous grain structure[1]. DRX originates at high angle grain boundaries (HABs)[2] which may pre-exist in the structure or is formed during straining. The local bulging of grain boundaries is frequently observed as the initial step to the nucleation of DRX and is often termed as strain induced grain boundary migration (SIBM)[3].

DRX is very important from an industrial point of view because it is a common microstructural phenomenon during the actual hot working processes of many metals such as stainless steels[4–7]. Determining the required strains for the initiation and completion of DRX helps to more accurately design an industrial process, such as hot forging or rolling. It is well-known that the build-up of dislocation density during hot working reaches a critical value when grain boundaries start to bulge through SIBM[2]. SIBM happens at a critical strain quite close to the peak strain of the DRX flow curve[8]. Locally bulged boundaries sweep away dislocations and cause a drop in the work hardening rate which was already under the control of dynamic recovery[9]. Based on this process, Poliak and Jonas[10–13] determined the critical strain as the inflection point of work hardening *vs* flow stress. After the critical point, the local bulges in boundaries grow to occupy the prior boundaries and form the so-called "necklace structure" at the peak[8]. The kinetics of DRX beyond the peak determines the strain required to reach the steady state flow. It is therefore evident that the critical peak and steady state strains are essential in characterizing the DRX behavior of a certain alloy. Although the concept of DRX has been well documented and characteristic strains have been correlated to the processing variable in many alloys, the DRX behavior of some special materials needs to

† Corresponding author. Prof., Ph.D.; Tel.: +98 511 8805115; Fax: +98 511 8763305; E-mail address: r.ebrahimi@ferdowsi.um.ac.ir, r_ebrahimi2000@yahoo.com (G.R. Ebrahimi).

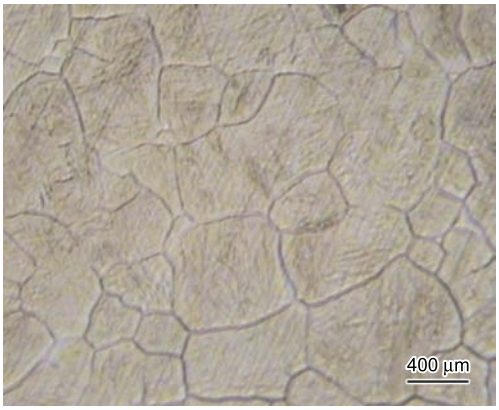

Fig. 1 Starting microstructure of the stainless steel used in this investigation

be further developed in order to increase the productivity of industrial hot working processes.

The goal of this investigation is therefore to analyze the DRX behavior of martensitic stainless steel, an area which did not receive much attention in the past. The studied alloy is widely used in high strength corrosion resistance applications and the actual information about hot working and DRX behavior of it is greatly solicited by hot forging and rolling plants.

2. Experimental

The chemical compositions of 13%Cr martensitic stainless steel used in this research is Cr 13.09, C 0.05, Si 0.8, Mn 1.00, S 0.003, P 0.025 and Fe balance (wt%). Cylindrical specimens, with a diameter of 8 mm and a height of 12 mm, were machined from the center of the as-received hot forged billet according to the ASTM E209 standard. The specimens were then solution treated at 1100 °C for 30 min before compression tests. The microstructure of annealed specimens consisted of equiaxed grains with an average grain size of 176 μm, as shown in Fig. 1.

In order to minimize the effect of friction and to keep the boron nitride as a lubricant between the contacting surfaces of samples and anvils, some concentric grooves of 0.5 mm depth were machined on the upper and lower surfaces of the samples. A Zwick/Roell 250 testing machine was used to perform the hot compression tests. Before testing, specimens were reheated to 1200 °C, held for 5 min then cooled down to test temperature. After soaking for 3 min, continuous hot compression tests were carried out in temperature ranges of 950–1100 °C and at strain rates of 0.001, 0.01 and 0.1 s^{-1}. The thermomechanical treatment schedule performed on specimens is shown in Fig. 2. The samples were quenched after hot compression to preserve the microstructure of DRX. The water-quenched specimens were polished with 1 μm of diamond paste and then etched in hot supersaturated picric acid to reveal the prior austenite grain boundaries on the longitudinal planes of the deformation

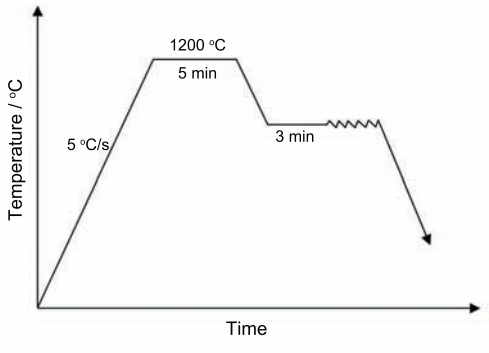

Fig. 2 Thermal and thermomechanical cycles imposed on samples in this research

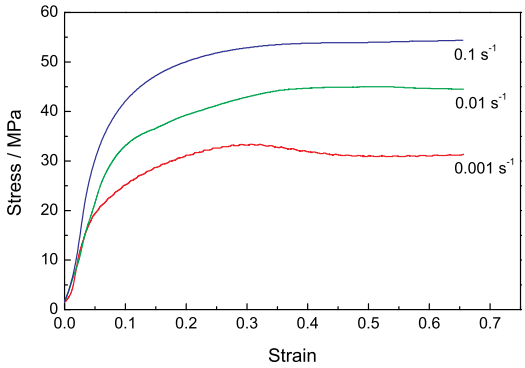

Fig. 3 True stress–true strain curves of specimens hot deformed at 950 °C and different strain rates

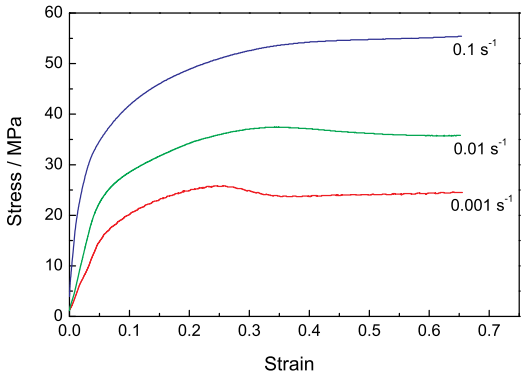

Fig. 4 True stress–true strain curves of specimens hot deformed at 1000 °C and different strain rates

specimens.

3. Results and Discussion

3.1 Effects of deformation conditions on flow curves

Flow curves obtained at different temperatures and strain rates are shown in Figs. 3–6. Most of the curves exhibit typical DRX behavior with a single peak stress followed by a gradual fall towards a steady-state stress. However, the peak becomes less obvious when the strain rate increases or the defor-

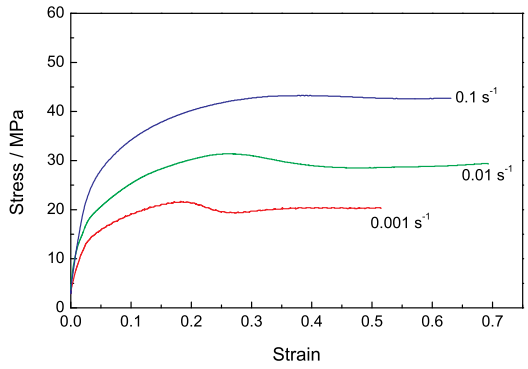

Fig. 5 True stress-true strain curves of specimens hot deformed at 1050 °C and different strain rates

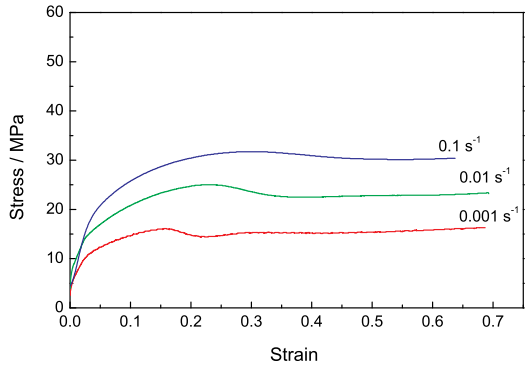

Fig. 6 True stress-true strain curves of specimens hot deformed at 1100 °C and different strain rates

mation temperature decreases.

The drop in flow stress due to the deformation temperature may be attributed to the increase in the rate of restoration processes and the decrease in the strain hardening rate. Since the formation of DRX nuclei becomes easier at higher deformation temperatures, the critical strain for the initiation of DRX gets lower. Moreover, the mobility of grain boundaries grows with higher deformation temperatures and hence the rate of DRX rises. Therefore, both the peak and steady-state strains decrease with higher deformation temperatures. The correlating increase in the flow stress and strain rate can be ascribed to the decline in the rate of restoration processes and the rise in the strain hardening rate. The rate of dynamic recovery (DRV) also falls with increasing strain rates. The srain during hot working needs to reach a critical value to develop the substructure which has a key influence on the formation of a DRX nucleus. Moreover, as the mobility of grain boundaries diminishes with a rising strain rate, peak and steady-state strains increase.

3.2 Hot deformation characteristics

Several empirical equations have been proposed to determine the deformation activation energy of steels.

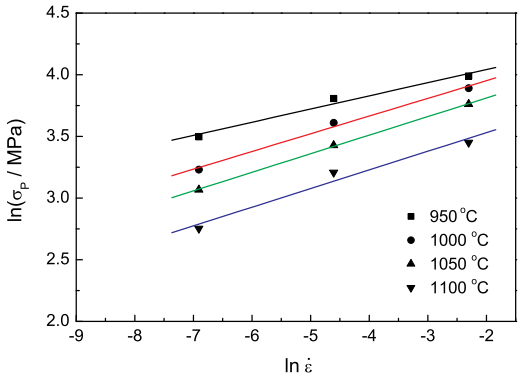

Fig. 7 Effect of strain rate on the peak stress at constant temperature

The most frequently used one is as follows[9]:

$$\sigma_{\mathrm{p}} = A \cdot Z^q = A \cdot [\dot{\varepsilon}\exp(Q/RT)]^q \tag{1}$$

where σ_{p} is the peak stress, A is a constant depending on chemical composition and initial austenite grain size, Z is the Zener–Hollomon parameter, $\dot{\varepsilon}$ is the strain rate, Q is the activation energy of deformation, R is the gas constant, T is the absolute temperature and q is a constant. Taking natural logarithm of both sides of Eq. (1) the expression for peak stress is given as:

$$\ln\sigma_{\mathrm{p}} = \ln A + q\ln(\dot{\varepsilon}) + qQ/RT \tag{2}$$

From Eq. (2) it can be seen that, when the deformation temperature is constant, the variation of peak stress with the strain rate is linearly fitted. Therefore, the value of q can be obtained as follows:

$$q = [\delta \ln \sigma_{\mathrm{p}}/\delta \ln \dot{\varepsilon}]_T \tag{3}$$

According to Eq. (3), the power law exponent q can be determined from the slope of the plot of the peak stress *vs* strain rate at a constant temperature, as shown in Fig. 7, q takes the value of 0.13 for the studied steel. At a constant strain rate, one can take the partial derivative of Eq. (2), with respect to the inverse deformation temperature, to obtain the apparent activation energy as follows:

$$[\delta \ln \sigma_{\mathrm{p}}/\delta(1/T)]_{\dot{\varepsilon}} = qQ/R \tag{4}$$

According to Eq. (4), the activation energy of deformation Q can be determined from the slope of the plot of peak stress against the reciprocal of temperature at a constant strain rate, as shown in Fig. 8. The obtained value of Q is about 413 kJ/mol. Therefore, the peak stress of the DRX flow curve in the present steel can be expressed as:

$$\sigma_{\mathrm{p}} = 0.097 \cdot Z^{0.13} = 0.097 \cdot [\dot{\varepsilon} \cdot \exp(413000/RT)]^{0.13} \tag{5}$$

For the hot flow curves given in Figs. 3–6, the true stress-true strain data were used to calculate the values of the strain hardening rate (θ=dσ/dε). The

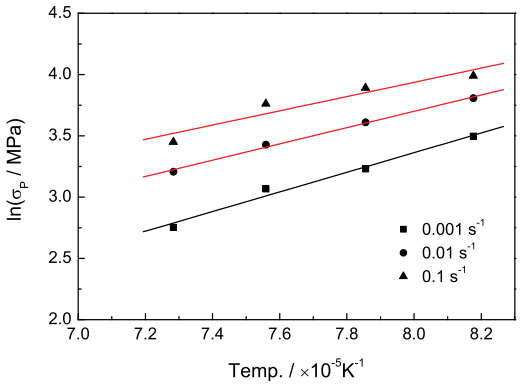

Fig. 8 Effect of temperature on the peak stress at constant strain rate

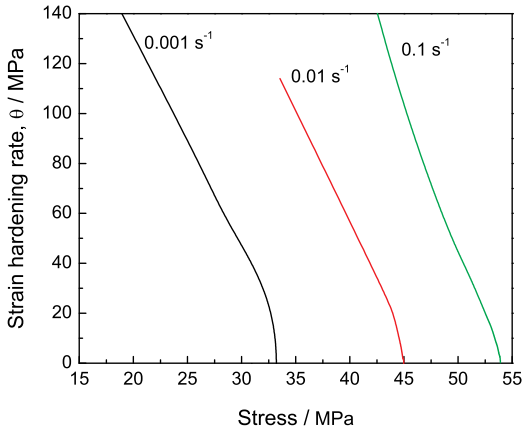

Fig. 9 $\theta-\sigma$ curves of hot deformed steel at 950 °C and different strain rates

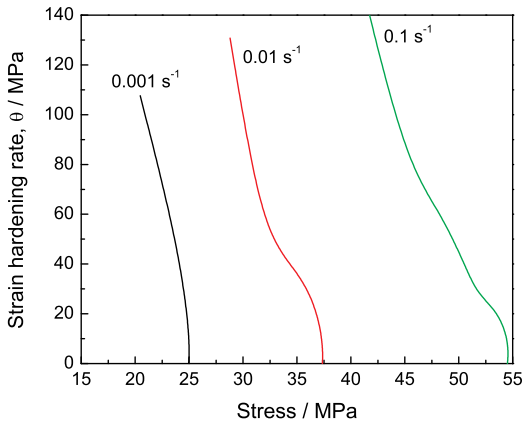

Fig. 10 $\theta-\sigma$ curves of hot deformed steel at 1000 °C and different strain rates

strain hardening rate values were then plotted as a function of the flow stress (Figs. 9–12). According to the approach of Poliak and Jonas[10–13], σ_p is represented in the θ–σ curves of the point at which the strain hardening rate equals zero (θ=0). The inflection point of θ–σ curves indicates the critical stress (σ_c) for the initiation of DRX.

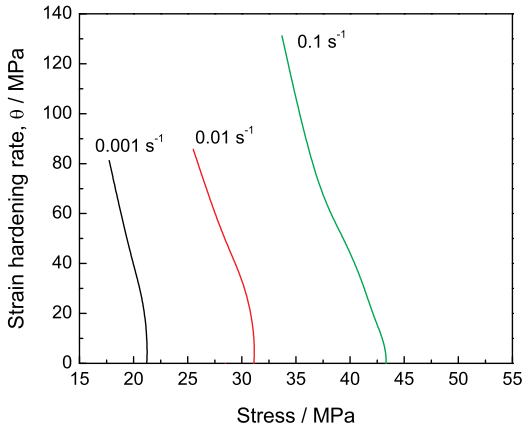

Fig. 11 $\theta-\sigma$ curves of hot deformed steel at 1050 °C and different strain rates

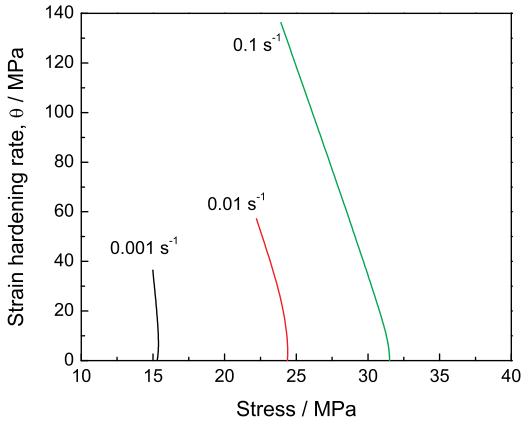

Fig. 12 $\theta-\sigma$ curves of hot deformed steel at 1100 °C and different strain rates

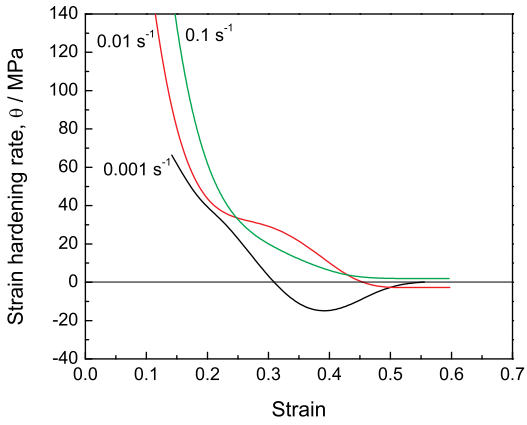

Fig. 13 Strain hardening rate *vs* strain for steel deformed at 950 °C and different strain rates

The strain hardening rate was plotted as a function of the true strain at different deformation temperatures and strain rates, as shown in Figs. 13–16. This was to find the strain at which the rate of dynamic softening is maximized. The minimum points in

Table 1 Calculated DRX parameters of steel deformed at different deformation conditions

Temp./°C	Strain rate	ε_c	ε_p	ε^*	σ_c	σ_p
950	0.001	0.21	0.32	–	25	33
	0.01	0.26	0.46	–	34	45
	0.1	0.47	0.51	–	41	60
1000	0.001	0.18	0.27	0.30	19	25.3
	0.01	0.22	0.35	0.42	28	37
	0.1	0.35	0.46	0.51	37	55
1050	0.001	0.14	0.18	0.24	16	21.5
	0.01	0.18	0.27	0.36	23	32
	0.1	0.30	037	0.45	33	44
1100	0.001	0.10	0.16	0.21	12	15.7
	0.01	0.14	0.23	0.31	19	24.7
	0.1	0.22	0.32	0.41	24	31.5

Note: subscripts "C" and "P" refer to critical and peak, respectively

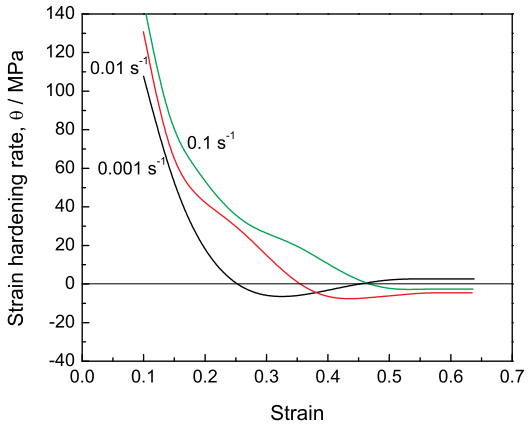

Fig. 14 Strain hardening rate *vs* strain for steel deformed at 1000 °C and different strain rates

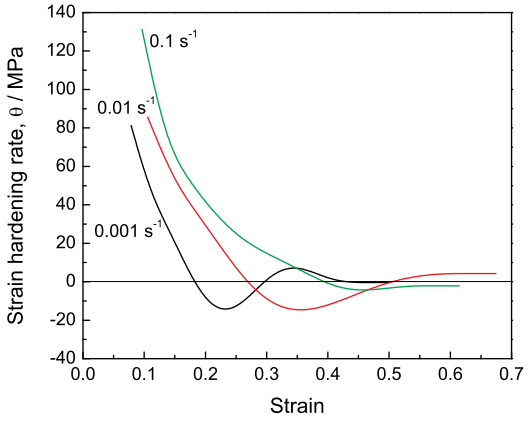

Fig. 15 Strain hardening rate *vs* strain for steel deformed at 1050 °C and different strain rates

these plots represent the strains at which the rate of dynamic softening is maximized, ε^*[14,15]. It is seen that the value of ε^* increases with decreasing deformation temperatures and increasing strain rates. In addition, after this minimum point, the strain hardening rate increases and reaches zero as the steady state deformation is attained. Therefore, the steady-state strain can be defined from θ–ε curves. From θ–ε plots, it is inferred that dynamic recrystallization is completed under the studied deformation conditions. However, at deformation

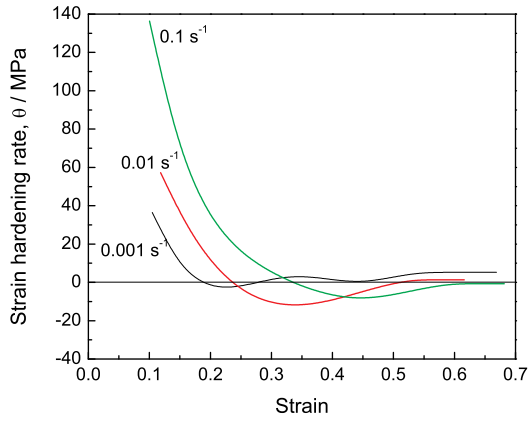

Fig. 16 Strain hardening rate *vs* strain for steel deformed at 1100 °C and different strain rates

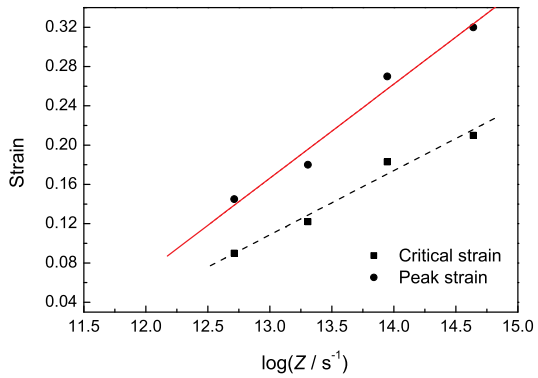

Fig. 17 Effect of deformation condition (Z parameter) on peak and critical strain

temperatures of 950 and 1000 °C and strain rates of 0.1 and 0.01 s^{-1}, dynamic recrystallization is partial due to the fact that the strain hardening rate does not reach zero at the end of deformation.

The calculated DRX parameters are listed in Table 1. The dependence of the critical and peak strain and stress of the present steel under different deformation conditions (different Z values) are shown in Figs. 17 and 18. It can be seen that the peak and critical stress and strain of DRX increase with a higher Z parameter. The ratio of $\varepsilon_c/\varepsilon_p$ and σ_c/σ_p are nearly constant as 0.68 and 0.77, respectively. Therefore,

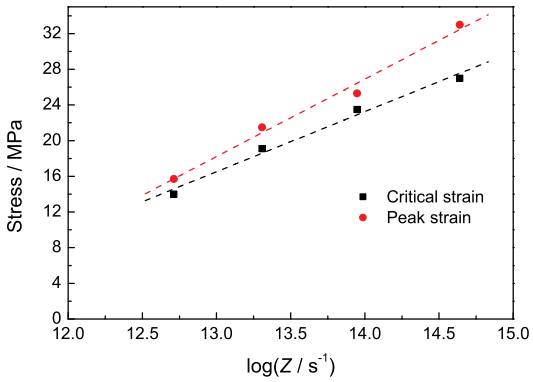

Fig. 18 Effect of deformation condition (Z parameter) on peak and critical stress

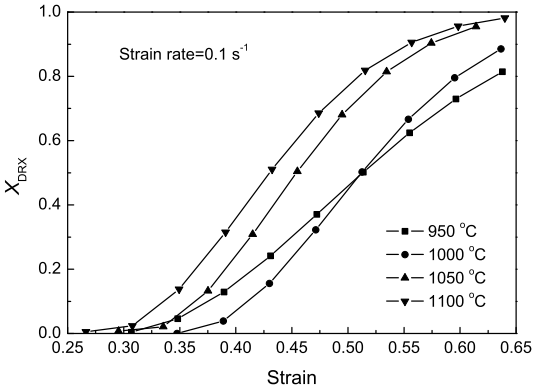

Fig. 19 Predicted volume fraction of dynamic recrystallization obtained under different temperatures at constant strain rate of 0.1

there is a linear relationship between the critical characteristics of DRX and Z, as given by the following equations:

$$\varepsilon_c = 0.00028 \cdot Z^{0.45},\ \sigma_c = 0.20 \cdot Z^{0.33} \quad (6)$$

$$\varepsilon_p = 0.0006 \cdot Z^{0.43},\ \sigma_p = 0.145 \cdot Z^{0.37} \quad (7)$$

The dependence of peak stress and strain on temperature and strain rates confirms that deformation is controlled by a thermally activated process[10,11].

3.3 DRX kinetics

The volume fraction of DRX can be described using an Avrami type model as follows[16]:

$$X_{DRX} = 1 - \exp[-0.693(\varepsilon - \varepsilon_c)/\varepsilon^*)^2] \quad (8)$$

Where, X_{DRX} is the DRX fraction, ε is the true strain, ε_c is the critical strain for the onset of DRX, and ε^* is the strain for the maximum softening rate during dynamic recrystallization. When this model is applied to the present data, the volume fraction of DRX, as a function of strain at different deformation temperatures with a constant strain rate of 0.1, is shown in Fig. 19. It is evident that the volume fraction

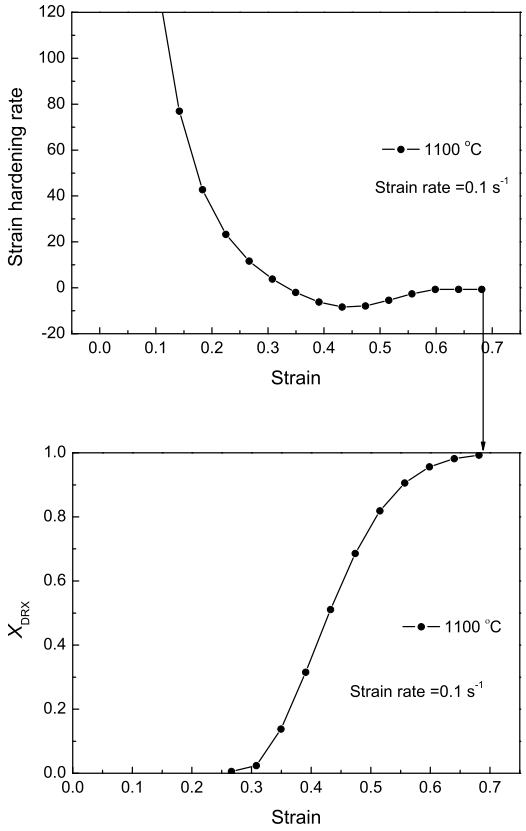

Fig. 20 Coincidence of predicted steady state strain with strain hardening rate (θ=0) and with the model used for calculation of recrystallized fraction (X_{DRX}=100%)

of dynamic recrystalliztion increases with strain beyond ε_c and reaches unity at the steady state strain. In addition, the strain required for the same amount of recrystallized fractions increases with decreasing deformation temperatures. Compared to higher temperatures, at the deformation temperature of 950 °C, DRX is delayed and requires higher strain.

The onset of steady-state deformation can be identified using the plot of strain hardening rate *vs* strain (Figs. 13–16). The second point at which the strain hardening rate reaches zero corresponds to the onset of steady-state flow. In Fig. 20, the strain hardening rate and recrystallized fraction are both plotted against strain at a strain rate of 0.1 s^{-1} and a temperature of 1100 °C. Fig. 20 confirms the accuracy of the model used to predict the dynamically recrystallized volume fraction. It is clear that the onset of steady-state deformation calculated from strain hardening rate data (θ=0) coincides with the point at which the DRX fraction determined by the Avrami-type model reaches unity.

4. Conclusions

In the present research, the dynamic recrystallization behavior of 13%Cr martensitic stainless steel was investigated using hot compression tests. The main

results can be summarized as follows:

Over a temperature range of 950–1100 °C and at strain rate range of 0.001–0.1 s^{-1}, the constitutive equation of peak flow behavior of this steel was developed.

The deformation activation energy of austenite was calculated to be about 413 kJ/mol. The important parameters of DRX were determined such as the critical strain for DRX initiation (by the Poliak and Jonas method), the peak strain, the strain associated with the maximum rate of dynamic softening, the steady-state strain and the peak stress calculated from true stress-true strain and strain hardening rate data.

The critical strain and strain of maximum softening rate were used to predict the kinetics of dynamic recrystallization. The Avramy-type expression was successfully applied to the model of dynamic recrystallization kinetics.

REFERENCES

[1] F. Montheillet and J.J. Jonas: *Encycl. Appl. Phys.*, 1996, **16**, 205.
[2] F.J. Humphreys and M. Hatherly: *Recrystallization and Related Annealing, Phenomena*, 2nd edn, ELSEVIER, Oxford, 2004, 427.
[3] I. Saunders and J. Nutting: *Met. Sci.*, 1984, **18**, 571.
[4] A. Momeni, K. Dehghani, H. Keshmiri and G.R. Ebrahimi: *Mater. Sci. Eng. A*, 2010, **527**, 1605.
[5] A. Dehghan-Manshadi, M.R. Barnett and P.D. Hodgson: *Mater. Sci. Eng. A*, 2008, **485**, 664.
[6] A. Momeni, A. Shokuhfar and S.M. Abbasi: *J. Mater. Sci. Technol.*, 2007, **23**, 775.
[7] N.D. Ryan and H.J. McQueen: *Can. Metall. Quart.*, 1990, **29**, 147.
[8] G.R. Ebrahimi, H. Keshmiri, A. Momeni and M. Mazinani: *Mater. Sci. Eng. A*, 2011, **528**, 7488.
[9] A. Momeni, K. Dehghani and G.R. Ebrahimi: *J. Alloy. Compd.*, 2011, **509**, 9387.
[10] E.I. Poliak and J.J. Jonas: *ISIJ Int.*, 2003, **43**, 684.
[11] E.I. Poliak and J.J. Jonas: *Acta Mater.*, 1996, **44**, 127.
[12] E.I. Poliak and J.J. Jonas: *ISIJ Int.*, 2003, **43**, 692.
[13] J.J. Jonas and E.I. Poliak: *Mater. Sci. Forum,* 2003, **426–432**, 57.
[14] G.R. Stewart, A.M. Elwazri, S. Yue and J.J. Jonas: *Mater. Sci. Technol.*, 2006, **22**, 519.
[15] A. Momeni, K. Dehghani, G.R. Ebrahimi and H. Keshmiri: *Metall. Mater. Trans. A*, 2010, **41**, 2898.
[16] G.E. Dieter, H.A. Kuhn and S.L. Semiatin: *Handbook of Workability and Process Design*, ASM, Materials Park, Ohio, 2003, 35.